

# Structural determinants of monohydroxylated bile acids to activate $\beta_1$ subunit-containing BK channels<sup>S</sup>

Anna N. Bukiya,\* Jacob McMillan,<sup>†</sup> Abby L. Parrill,<sup>†</sup> and Alejandro M. Dopico<sup>1,\*</sup>

Department of Pharmacology,\* The University of Tennessee Health Science Center, Memphis, TN 38163; and Department of Chemistry and Computational Research on Materials Institute,<sup>†</sup> University of Memphis, Memphis, TN 38152

**Abstract** Lithocholate (LC) (10–300  $\mu$ M) in physiological solution is sensed by vascular myocyte large conductance, calcium- and voltage-gated potassium (BK) channel  $\beta_1$  accessory subunits, leading to channel activation and arterial dilation. However, the structural features in steroid and target that determine LC action are unknown. We tested LC and close analogs on BK channel (pore-forming *cbv1*+ $\beta_1$  subunits) activity using the product of the number of functional ion channels in the membrane patch (N) and the open channel probability (Po). LC (5 $\beta$ -cholanic acid-3 $\alpha$ -ol), 5 $\alpha$ -cholanic acid-3 $\alpha$ -ol, and 5 $\beta$ -cholanic acid-3 $\beta$ -ol increased NPo (EC<sub>50</sub> ~45  $\mu$ M). At maximal increase in NPo, LC increased NPo by 180%, whereas 5 $\alpha$ -cholanic acid-3 $\alpha$ -ol and 5 $\beta$ -cholanic acid-3 $\beta$ -ol raised NPo by 40%. Thus, the  $\alpha$ -hydroxyl and the *cis*-A-B ring junction are both required for robust channel potentiation. Lacking both features, 5 $\alpha$ -cholanic acid-3 $\beta$ -ol and 5-cholanic acid-3 $\beta$ -ol were inactive. Three-dimensional structures show that only LC displays a bean shape with clear-cut convex and concave hemispheres; 5 $\alpha$ -cholanic acid-3 $\alpha$ -ol and 5 $\beta$ -cholanic acid-3 $\beta$ -ol partially matched LC shape, and 5 $\alpha$ -cholanic acid-3 $\beta$ -ol and 5-cholanic acid-3 $\beta$ -ol did not. Increasing polarity in steroid rings (5 $\beta$ -cholanic acid-3 $\alpha$ -sulfate) or reducing polarity in lateral chain (5 $\beta$ -cholanic acid 3 $\alpha$ -ol methyl ester) rendered poorly active compounds, consistent with steroid insertion between  $\beta_1$  and bilayer lipids, with the steroid-charged tail near the aqueous phase. **■** Molecular dynamics identified two regions in  $\beta_1$  transmembrane domain 2 that meet unique requirements for bonding with the LC concave hemisphere, where the steroid functional groups are located.—Bukiya, A. N., J. McMillan, A. L. Parrill, and A. M. Dopico. **Structural determinants of monohydroxylated bile acids to activate  $\beta_1$  subunit-containing BK channels.** *J. Lipid Res.* 2008. 49: 2441–2451.

**Supplementary key words** steroids • protein-ligand interaction • computational modeling • maxiK channel • vascular smooth muscle • vasodilation

This work was supported by National Institutes of Health Grant HL-77424 (A.M.D.). A.L.P. gratefully acknowledges the Chemical Computing Group for the MOE software license.

Manuscript received 30 May 2008 and in revised form 14 July 2008.

Published, JLR Papers in Press, June 23, 2008.  
DOI 10.1194/jlr.M800286-JLR200

Copyright © 2008 by the American Society for Biochemistry and Molecular Biology, Inc.

This article is available online at <http://www.jlr.org>

Upon activation, voltage- and  $\text{Ca}^{2+}$ -gated  $\text{K}^+$  channels of large conductance (BKs) generate  $\text{K}^+$  outward currents, which tend to hyperpolarize the membrane potential and thus, negatively feed back on depolarization-induced  $\text{Ca}^{2+}$  influx. In vascular smooth muscle, this BK channel-mediated negative feedback mechanism serves to control myogenic tone and favors relaxation (1, 2). A wide variety of physiologically relevant steroids, including estrogens, androgens, mineralo- and glucocorticoids, and bile acids, increase BK channel activity (3–5), a mechanism that might contribute to nongenomic modulation of myogenic tone. In particular, lithocholate (LC) and other bile acids, at aqueous concentrations ranging from 10 to 300  $\mu$ M, are highly effective activators of BK channels (4, 6). This action can explain or at least contribute to the well-known vasodilating properties and hyperkinetic circulation induced by bile acids in human pathophysiology (7). In a wide variety of human pathological conditions (8–12), a significant spillover of bile acids from the portal to the systemic circulation occurs, resulting in 10- to 100-fold (even close to 1 mM) higher systemic bile acid concentrations (11, 13, 14). These levels are within and even above the concentrations of bile acids reported to enhance vascular myocyte BK<sub>Ca</sub> channel activity (4).

In hepatobiliary disease, there may be not only an overall increase in systemic bile acid levels, but also a change in composition. In particular, free and conjugated LC levels, which normally constitute 5–10% of total bile acids, can dramatically increase in liver disease (11).

Among naturally occurring bile acids, the monohydroxylated LC is remarkably effective in increasing vascular myocyte BK channel activity (4), which is consistent with the powerful smooth muscle relaxant properties of

Abbreviations: BK, large conductance, calcium- and voltage-gated potassium; CMC, critical micellar concentration; LC, lithocholate; N, number of functional ion channels in the membrane patch; Po, open channel probability; RMSG, root mean square gradient; TM2, transmembrane domain 2.

<sup>1</sup>To whom correspondence should be addressed.

e-mail: [adopico@utmem.edu](mailto:adopico@utmem.edu)

**S** The online version of this article (available at <http://www.jlr.org>) contains supplementary data in the form of five figures.

hydrophobic bile acids (15). We have demonstrated that LC-induced vasodilation is largely endothelium-independent, and blunted after genetic ablation of *KCNMB1* (6). This gene codes for the BK channel accessory subunit of the  $\beta_1$  type, which is particularly abundant in smooth muscle (16). Moreover, studies with recombinant BK channels in cell-free membrane patches demonstrate that co-expression of accessory  $\beta_1$  subunits is necessary for LC to increase the activity of BK channel complexes that include pore-forming subunits (cbv1; AY330293) cloned from arterial myocytes (6). Notably, channel accessory subunits of the  $\beta_4$  type, which prevail in nervous tissue, fail to render the BK channel complex sensitive to LC (6). Furthermore, recent data from BK channels that include  $\beta_1$ - $\beta_4$  chimeric subunits demonstrate that the  $\beta_1$  transmembrane domain 2 (TM2) distinctly behaves as a bile acid-sensing element (17). Whether  $\beta_1$  TM2 provides a docking area that allows selective interaction with LC, a structural hypothesis for this steroid effectiveness on channel function, remains unknown.

Structural specificity in protein binding sites requires defined structural determinants in the ligand molecule. Previous studies indicate that the overall hydrophobicity of the steroid nucleus and “planar polarity” of the molecule, i.e., the existence of distinct hydrophobic and hydrophilic sides or hemispheres in a rigid amphiphile (18, 19), favored BK channel activation by naturally occurring bile acids (4). However, the specific structural determinants that make LC such a highly effective activator of BK channels remain to be identified.

Using a combination of computational simulations and single-channel, patch-clamp electrophysiology on recombinant BK channels cloned from vascular smooth muscle (cbv1 pore-forming + accessory  $\beta_1$  subunits), the current study pinpoints the specific structural determinants in the steroid molecule that are necessary for the naturally occurring LC and related analogs to activate BK channels. In addition, we postulate a structural model(s) of LC insertion in the  $\beta_1$  TM2-bilayer interface and docking onto specific  $\beta_1$  TM2 regions, which explains the differential efficacy of bile acids on BK channel activity. This information provides critical insight for designing LC-based pharmacophores to select novel and effective vasodilators that target smooth muscle BK channels.

## METHODS

### cRNA preparation and injection into *Xenopus* oocytes

Full-length cDNA coding for cbv1-subunits (AY330293) was cloned from rat cerebral artery myocytes by PCR and ligated to the PCR-XL-TOPO cloning vector (Invitrogen, Carlsbad, CA). Cbv1 cDNA was then cleaved by BamHI (Invitrogen) and XhoI (Promega, Madison, WI), and directly inserted into the pOX vector for expression in *Xenopus* oocytes. pOX-cbv1 was linearized with NotI (Promega) and transcribed in vitro using T3 polymerase. BK  $\beta_1$  cDNA inserted into the EcoR I/Sal I sites of the pCIneo expression vector was linearized with NotI and transcribed in vitro using T7 polymerase. The mMessage-mMachine kit (Ambion, Austin, TX) was used for transcription. The pOX vector and the BK  $\beta_1$  cDNA were generous gifts from Aguan Wei

(Washington University, Saint Louis, MO) and Maria Garcia (Merck Research Laboratories, Whitehouse Station, NJ), respectively.

Oocytes were removed from *Xenopus laevis* (NASCO, Fort Atkinson, WI; Xenopus Xpress, Plant City, FL) and prepared as described elsewhere (20). cRNA was dissolved in diethyl polycarbonate-treated water at 5 (cbv1) and 15 ( $\beta_1$ ) ng/ $\mu$ l; 1  $\mu$ l aliquots were stored at  $-70^\circ\text{C}$ . Cbv1 cRNA (2.5 ng/ $\mu$ l) was co-injected with  $\beta_1$  (7.5 ng/ $\mu$ l) cRNA, giving molar ratios  $\geq 6:1$  ( $\beta:\alpha$ ). cRNA injection (23 nl/oocyte) was conducted using a modified micropipette (Drummond, Broomall, PA). The interval between injection and patch-clamp recordings was 48–72 h.

### Electrophysiology data acquisition

Oocytes were prepared for patch-clamp recordings as described (20). Currents were recorded from inside-out (I/O) patches. Both bath and electrode solutions contained (mM): 135  $\text{K}^+$  gluconate, 5 EGTA, 2.28  $\text{MgCl}_2$ , 5.22  $\text{CaCl}_2$ , 15 HEPES, 1.6 HEDTA, pH 7.35. In all experiments, the free  $\text{Ca}^{2+}$  in solution was adjusted to 10  $\mu\text{M}$  by adding  $\text{CaCl}_2$ . Free  $\text{Ca}^{2+}$  was calculated with MaxChelator Sliders (Stanford University, Palo Alto, CA) and validated experimentally using  $\text{Ca}^{2+}$ -selective and reference electrodes (Corning Inc., Corning, NY).

Patch-recording electrodes were made as previously described (20). An agar bridge with gluconate as the main anion was used as the ground electrode. After excision from the oocyte, the membrane patch was exposed to a stream of bath solution containing each agent at final concentration. Solutions were applied onto the cytosolic side of the membrane patch using a pressurized, automated DAD12 system (ALA, New York, NY) via a micropipette tip with an internal diameter of 100  $\mu\text{m}$ . Experiments were carried out at room temperature ( $21^\circ\text{C}$ ).

Currents were recorded using an EPC8 amplifier (HEKA, Lambrecht/Pfalz, Germany) at 1 kHz using a low-pass, eight-pole Bessel filter (Frequency Devices 902LPF, Haverhill, MA). Data were digitized at 5 kHz using a Digidata 1320A A/D converter and pCLAMP 8.0 (Molecular Devices, Haverhill, MA). As index of channel steady-state activity, we used the product of the number of functional ion channels in the membrane patch [N] and the open channel probability (Po). NPo was obtained from all-points amplitude histograms (21) from  $\geq 30$  s of continuous recording under each experimental condition.

### Chemicals and compound perfusion

LC and its structural analogs (Fig. 1), with the exception of  $5\alpha$ -cholanic acid  $3\beta$ -ol (epialloLC), were purchased from Steraloids (Newport, RI). EpialloLC was generously provided by Dr. Takashi Iida (Nihon University, Tokyo, Japan). All other chemicals were purchased from Sigma (St. Louis, MO). On the day of the experiment, a stock solution (333 mM) of each cholane derivative (LC or analog) was freshly made in DMSO by sonication for 5 min. For electrophysiological recordings, the cholane-containing stock solution was diluted 1/10 in 95% ethanol, and further diluted with bath solution to final cholane concentrations (3–1,000  $\mu\text{M}$ ). The DMSO-ethanol vehicle in bath solution ( $\leq 0.1/\leq 0.86\%$  final concentrations) was used as control perfusion.

For LC and analogs, both chemical and common names are given when first used (the latter in parenthesis). Then, common names (when available) are used throughout the manuscript.

### Electrophysiology data analysis

Data are expressed as mean  $\pm$  SEM; n = number of patches. NPo changes in response to perfusion with cholane-containing solution are shown as percentage of control, which was the NPo obtained under control perfusion (see above) immediately before applying cholane-containing solution. Data were analyzed

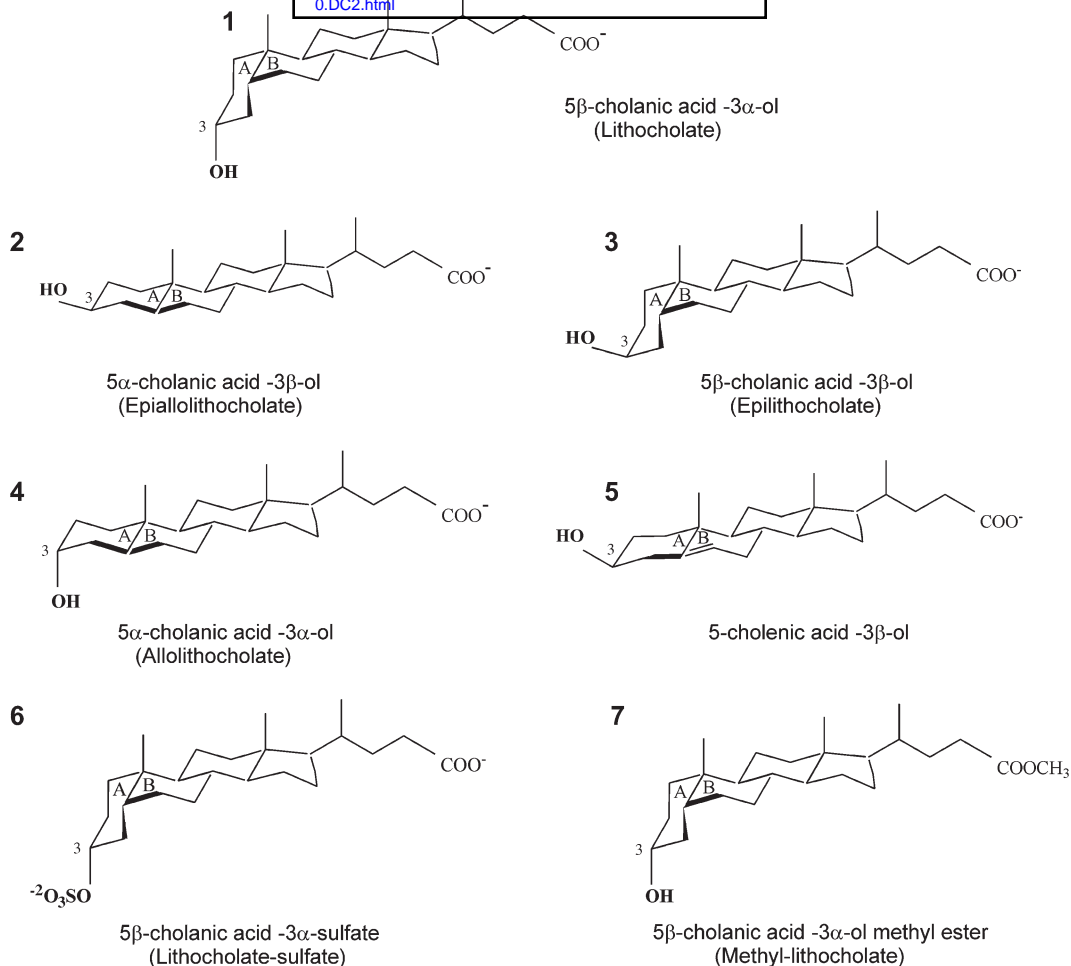


**Fig. 1.** Molecular structures of lithocholate (LC) and its derivatives. In all structures (except number 7) the free carboxyl group ( $pK_a = 5$ ) at the end of the lateral chain is shown in its ionized form, which predominates in our experimental conditions ( $pH\ 7.4$ ). In all panels, both chemical and trivial (when appropriate) names are provided.

with pCLAMP 8.0 (Molecular Devices). Further analysis, plotting, and fitting were conducted using Origin 7.0 (Originlab, Northampton, MA) and InStat 3.0 (GraphPad Software, San Diego, CA). Statistical analysis was conducted using one-way ANOVA and Bonferroni's multiple comparison test; significance was set at  $P < 0.05$ .

### Computer modeling of steroid structures

Three-dimensional structures of LC and its structural analogs were modeled using Molecular Operating Environment (MOE) software (Chemical Computing Group, Montreal, Canada). Models were constructed in ionized states, which should be predominant at  $pH\ 7.4$ , and optimized with the MMFF94 forcefield (14) to a root mean square gradient (RMSG) of  $0.1\ kcal\cdot mol^{-1}\cdot\text{Å}^{-1}$  (22). Conformations of LC were generated using the stochastic conformational search routine in MOE, with default dielectric settings equivalent to gas-phase. The conformational preferences in the low-dielectric lipid environment were expected to be similar. Structural analogs were flexibly aligned onto the lowest energy conformation of LC.

### Computer modeling of steroid-BK $h\beta_1$ complexes

The polypeptide extending from residue Q155 to S179, which contains the BK  $h\beta_1$  second transmembrane domain

(TM2, residues A156-V178; 9) was modeled as an ideal  $\alpha$  helix, and optimized with the AMBER99 forcefield to an RMSG of  $0.1\ kcal\cdot mol^{-1}\cdot\text{Å}^{-1}$  (23). The dielectric constant for this model was set as 3, this value being appropriate for the lipid membrane interior (24). The lowest energy structure of LC was manually positioned with either its C3 hydroxyl near T165 and its C24 carboxyl facing the extracellular aqueous medium or its C3 hydroxyl near T169 and its C24 carboxyl facing the intracellular aqueous medium. Single bonds in the acyclic chain of LC were rotated as needed to position the functional groups as described. These starting complexes were optimized to an RMSG of  $0.1\ kcal\cdot mol^{-1}\cdot\text{Å}^{-1}$ . Molecular dynamics simulations (1 ns) using 2 fs time steps at  $300^\circ K$  were performed to assess the stability and structural changes of each complex over time.

## RESULTS

A *cis* junction between rings A and B and the  $\alpha$  configuration of the C3 hydroxyl are both necessary for LC and analogs to robustly increase BK channel activity. The steroidal structure of LC (LC; compound 1 in Fig. 1) is characterized by: 1) a junction between rings A and B in *cis* configuration, which provides a bean shape to the steroidal

ring structure, and 2) a single polar group located in C3 and in  $\alpha$  configuration. This configuration ensures that the polar group has an axial orientation, that is, it points to the opposite side of the ring plane than the methyl groups (18) (Fig. 1). We first determined whether a *cis* junction between rings A and B and the  $\alpha$  configuration of the C3 hydroxyl are, indeed, necessary for LC activation of BK channels. To do so, we compared LC action on BK channel NPo with that of 5 $\alpha$ -cholanic acid-3 $\beta$ -ol, an LC analog with an A/B ring junction in *trans* configuration and its C3 hydroxyl in  $\beta$  configuration (epi*allo*LC or compound 2 in Fig. 1). Each compound was perfused onto the intracellular side of I/O membrane patches (see Methods), with a free  $\text{Ca}^{2+}_i$  set to 10  $\mu\text{M}$  and  $V_m = -20$  mV. These conditions of  $\text{Ca}^{2+}_i$  and voltage approach those faced by native BK channels in cerebral artery myocytes during contraction (25, 26). At a concentration of 150  $\mu\text{M}$ , which is the  $\text{EC}_{90}$  for LC to activate both native cerebral artery myocyte and recombinant (cbv1+ $\beta_1$ ) channels (6), epi*allo*LC routinely failed to modify BK channel activity (Fig. 2A, B). The difference between LC and epi*allo*LC persisted even when the two analogs were evaluated at concentrations as high as 300  $\mu\text{M}$  (Fig. 3), that is, close to their critical micellar concentration (CMC) under our ionic recording conditions ( $\leq 1$  mM) (4, 27). Application of epi*allo*LC or any other monohydroxylated bile acid (see below) at  $\geq 1$  mM routinely resulted in loss of the gigaohm recording seal, probably due to nonspecific membrane disruption caused by bile acid micelles (4). These data indicate that a *cis* junction between rings A and B and/or the  $\alpha$  configuration of the C3 hydroxyl are necessary for LC to increase BK channel activity.

To determine whether the two structural features in the LC steroidal ring considered above are both critical for LC action, we used two other monohydroxylated bile acids, each differing from LC in only one structural feature. The two compounds examined are 5 $\beta$ -cholanic acid-3 $\beta$ -ol (epiLC or compound 3 in Fig. 1) and 5 $\alpha$ -cholanic acid-3 $\alpha$ -ol (*allo*LC or compound 4 in Fig. 1). These structures differ from LC in either the C3 hydroxyl configuration (epiLC) or ring junction (*allo*LC). Under recording conditions identical to those used to probe LC and epi*allo*LC, 150  $\mu\text{M}$  epiLC or *allo*LC applied to the cytosolic side of I/O patches also caused a reversible activation of recombinant cbv1+ $\beta_1$  channels (Fig. 2A). However, the maximal increase in NPo ( $E_{\text{max}}$  or "efficacy") caused by epiLC (145% of control; Fig. 2B) or *allo*LC (141% of control; Fig. 2B) was considerably smaller ( $P < 0.05$ ) than that evoked by LC (epiLC  $E_{\text{max}}/\text{LC } E_{\text{max}} = 0.54$  and *allo*LC  $E_{\text{max}}/\text{LC } E_{\text{max}} = 0.52$ ). The effects of epiLC and *allo*LC are statistically similar ( $P > 0.05$ ). The results with epiLC on recombinant channels extend previous findings with vascular smooth muscle native BK channels showing that epiLC (100 and 333  $\mu\text{M}$ ) causes a reduced potentiation when compared with that evoked by LC (4). EpiLC and *allo*LC actions on recombinant cbv1+ $\beta_1$  channels were concentration-dependent, with potentiation of channel activity being smaller than evoked by LC at any given bile acid concentration, up to concentrations close to CMC (Fig. 3). These results in-

dicade that the hydroxyl configuration and *cis* junction between rings A and B are both required to ensure a robust activation of BK channels by LC and analogs. The presence of one of these structural features in the steroid molecule, however, suffices to evoke some channel activation by bile acids.

Although epiLC and *allo*LC greatly differed from LC in  $E_{\text{max}}$ , the three monohydroxylated bile acids increased BK channel steady-state activity with similar apparent affinities ( $\text{EC}_{50} = 43.5 \pm 5.9$ ,  $44.2 \pm 6.3$ , and  $48.6 \pm 5.8$   $\mu\text{M}$  for LC, *allo*LC, and epiLC, respectively;  $P > 0.05$ ) (Fig. 3; Table 1). This similarity appears to indicate that there are no significant differences in the access of these three analogs to a functional target(s) in the cell membrane.

### BK channel activation by monohydroxylated bile acids depends on the steroid molecular shape

The results shown in Figs. 2 and 3 indicate that the *cis* junction between rings A and B and the  $\alpha$  configuration of the C3 hydroxyl are both necessary for a robust activation of BK channels by LC. Epi*allo*LC, lacking both structural constraints, failed to modify channel activity, whereas epiLC and *allo*LC, having just one, caused some activation. Moreover, the structural determinant that appears to enable epiLC and *allo*LC to activate the BK channel is different for each of these analogs. Conceivably, BK channel activation by monohydroxylated bile acids is favored by molecular resemblance to LC. Thus, to begin to relate the differences in monohydroxylated bile acid efficacy for activating BK channels with the overall shape of the bile acid molecule, we constructed three-dimensional structures of LC and its structural analogs in the ionized state. The carboxylic acid group of unconjugated bile acids in aqueous solution has been reported to have apparent  $\text{pK}_a$ s ranging from 4.98 (for cholate at concentrations  $< \text{CMC}$ ) to 6.2 (for chenodeoxycholate in soluble micelles) (28, 29), which rise to  $\sim 7$  when bile acids are embedded within a proteolipid environment (29, 30). Our model of LC insertion in the membrane, however, proposes that the carboxylate in the steroid lateral chain is located in the aqueous face (pH 7.4) in close proximity to the membrane. Thus, although we do not dismiss a possible interaction between the channel receptor and bile acids in their nonionized carboxylic acid form (see Discussion), our steroid models were constructed considering that bile acids with ionized carboxylate groups predominate. Alignment of structural analogs to the lowest energy conformation of LC emphasizing the fit of polar functional groups during flexible superposition shows that only LC displays a molecular concave shape (including its movable side chain) with polar functional groups at the rim of the concave hemisphere. EpiLC and *allo*LC, which produce modest channel activation when compared with LC, can match the polar functional group positions of LC (Fig. 4A). However, an optimal match of the polar functional groups involved both conformational changes in the steroid A ring and reversed methyl group orientations relative to LC, which might compromise the ability of these compounds to induce the conformational

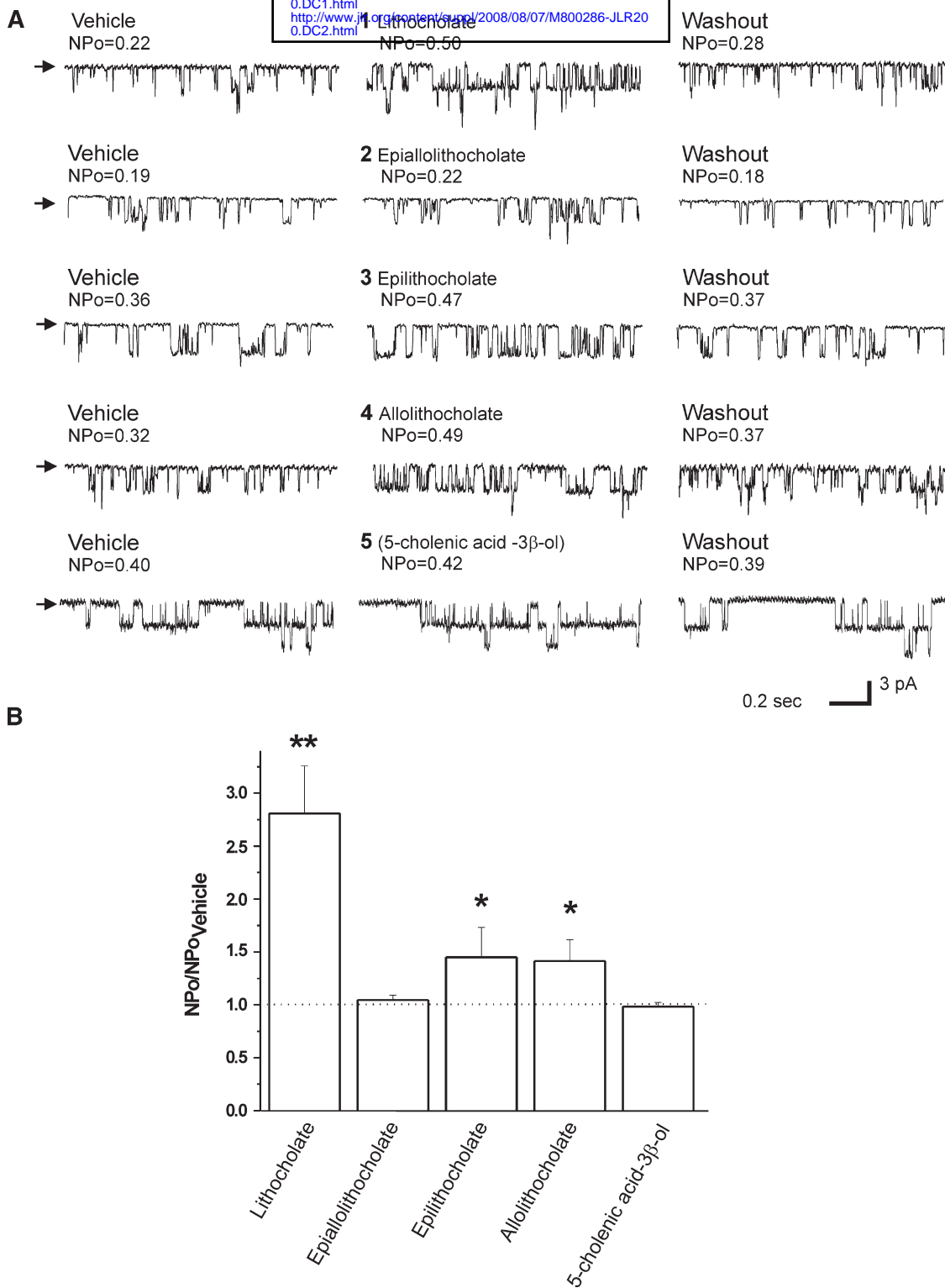


**Fig. 2.** Differential action of LC and derivatives on recombinant large conductance, calcium- and voltage-gated potassium (BK) (cbv1+ $\beta$ <sub>1</sub>) channels in inside-out (I/O) patches excised from *Xenopus laevis* oocytes. A: Representative single-channel records obtained at  $V_m = -20$  mV in symmetric  $Ca^{2+} = 10$   $\mu$ M. Arrows indicate baseline. Each compound (150  $\mu$ M) and vehicle was tested on the same patch; each compound-vehicle pair was tested on different patches excised from different oocytes. B: Averaged channel responses to LC and derivatives. \*  $P < 0.05$ ; \*\*  $P < 0.01$  vs. vehicle; n = 6 (LC), n = 6 (epialloLC), n = 4 (epiLC), n = 3 (alloLC), and n = 4 (5-cholenic acid-3 $\beta$ -ol).

change in their biomolecular target that gives maximal channel activation.

EpialloLC, which failed to activate BK channels at all concentrations tested (Figs. 2, 3), is unable to simulta-

neously match the acid- and hydrogen bond-accepting groups to LC conformation and shape (Fig. 4B). Finally, we investigated 5-cholenic acid-3 $\beta$ -ol (compound 5 in Fig. 1), where the ring unsaturation provides extra rigidity

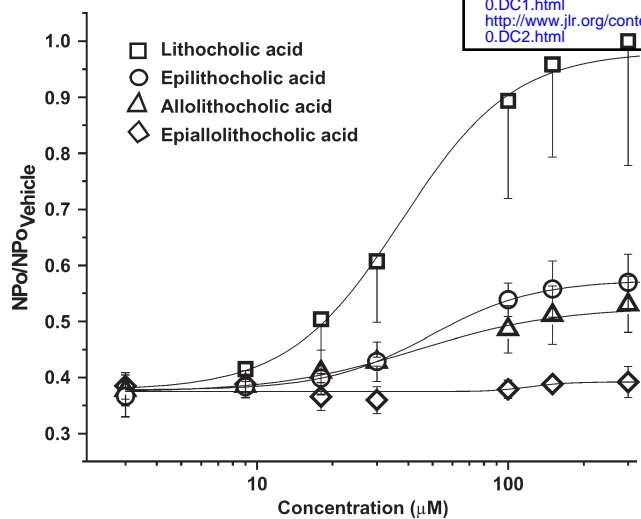


**Fig. 3.** Concentration-response curves for  $cbv1+\beta_1$  channel activation by LC and structural analogs. Data were obtained under conditions identical to those described for Fig. 2. Each data point represents the average response from no fewer than three membrane patches. Each average value was normalized to the maximum activation of BK channels by LC. Error bars indicate SEM.

to the A-B rings and a bend at the A-B ring junction that is intermediate between that formed by a *cis* A-B junction (found in LC and *epi*LC) and that formed by a *trans* A-B ring junction (found in *allo*LC and *epiallo*LC). This analog could overlap with LC in both the carboxylate region and the hydrogen bond acceptors (Fig. 4B). However, its rigid A/B ring structure cannot overlap with the concavity of LC (Fig. 4B). Application of 5-cholenic acid- $3\beta$ -ol (150  $\mu$ M) barely modified BK channel activity (Fig. 2A, B), which buttresses the importance of the bean shape of the bile acid molecule for activating BK channels. In synthesis, the two compounds that fail to overlap with the LC molecule also failed to activate the BK channel. Indeed, the ability of a monohydroxylated bile acid to activate the BK channel is a direct function of the analog structural match with the LC structure (see supplementary Fig. 1). Mismatch with LC, however, was primarily determined

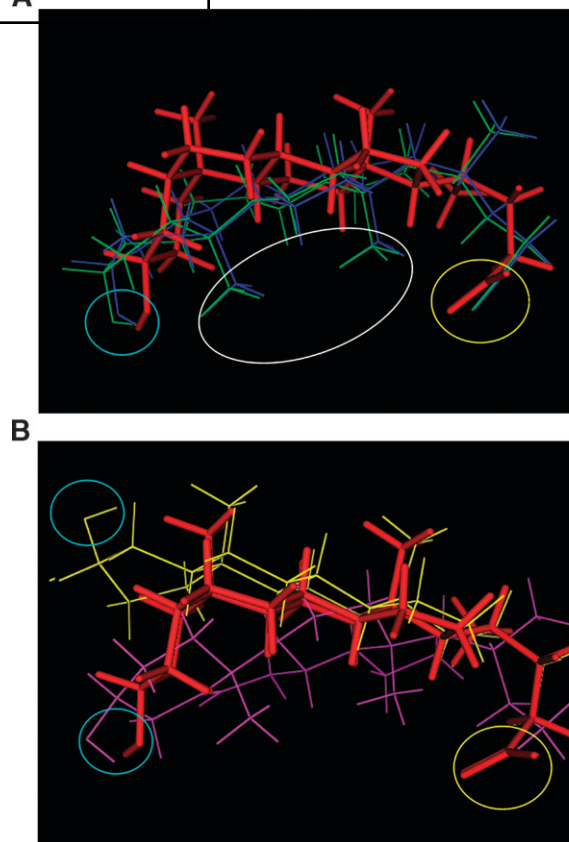


**Fig. 4.** Three-dimensional superposition of LC and analogs. A: Molecular structures of *allo*LC (navy lines), and *epi*LC (green lines) superposed onto the lowest energy conformation of LC (red sticks). The white oval shows that when the fit of polar functional groups is prioritized during the flexible superposition, the methyl groups in steroid nucleus of *epi*LC and *allo*LC are in the reverse direction to those of LC. This superposition shows that only LC displays a concave shape with polar functional groups at the rim of the concavity, although another two structures can successfully place their polar functional groups in a similar location. B: Structures of *epiallo*LC (yellow lines) and 5-cholenic acid- $3\beta$ -ol (purple lines) cannot be fully superposed onto the LC molecule (red sticks). While *epiallo*LC places its hydrogen bond acceptor away from the C3 hydroxyl of LC, 5-cholenic acid- $3\beta$ -ol cannot adopt fully bean-shaped conformation due to the presence of a double bond in the B-ring and, therefore, rigidity of the A/B ring junction. For panels A and B, yellow and blue circles emphasize overlap of acidic groups and hydrogen bond acceptors, respectively.

**TABLE 1.** Potency ( $EC_{50}$ ) and effectiveness ( $E_{max}$ ) of different monohydroxylated bile acids for activating BK ( $cbv1+\beta_1$ ) channels

| Compound                      | $EC_{50}$        | Maximum Effect |
|-------------------------------|------------------|----------------|
|                               | $\mu$ M          |                |
| Lithocholate                  | $43.53 \pm 5.95$ | $281 \pm 45$   |
| <i>Epi</i> allothocholate     | N/A              | $109 \pm 13$   |
| <i>Epilithocholate</i>        | $48.60 \pm 5.76$ | $145 \pm 28$   |
| <i>Allolithocholate</i>       | $44.21 \pm 6.28$ | $141 \pm 20$   |
| 5-Cholenic acid- $3\beta$ -ol | N/A              | $98 \pm 12$    |
| Lithocholate-sulfate          | $42.16 \pm 7.12$ | $153 \pm 23$   |
| Methyl-lithocholate           | N/A              | $119 \pm 11$   |

BK, large conductance, calcium- and voltage-gated potassium; N/A, non-applicable, because the analog was ineffective below critical micellar concentration. Half-maximal effective concentrations ( $EC_{50}$ s) were obtained from linear interpolation from concentration-response curves (Fig. 3). Maximal effect ( $E_{max}$ ) is shown as the increase in BK  $NPo$  as percent of control. For all compounds tested,  $E_{max}$  was obtained at 300  $\mu$ M in aqueous solution;  $n = 4-6$ . Data are shown as mean  $\pm$  SEM.

via different regions in the steroid molecule: the polar regions and the overall hydrophobic volume for *epiallo*LC and 5-cholenic acid- $3\beta$ -ol, respectively (**Table 2**). Collectively, these results indicate that small structural changes affecting the overall bean shape of the bile acid molecule drastically alter the efficacy of monohydroxylated bile acids in activating BK channels, and support the notion of a defined locus where the bile acid molecule should fit in order to stabilize a conformational change in their biomolecular target that results in increased channel activity.

#### Putative docking model between LC and BK $\beta_1$ subunits

We recently demonstrated that the BK  $\beta_1$  subunit TM2 is necessary for LC to activate BK channels. Moreover, it is

TABLE 2. RMSDs for heavy atoms and polar groups for different structural analogs when compared with the lithocholate molecule

| Molecular Structure           | RMSD         |              |
|-------------------------------|--------------|--------------|
|                               | Heavy Atoms  | Polar Groups |
|                               | $\text{\AA}$ |              |
| Lithocholate                  | 0            | 0            |
| Epilithocholate               | 2.2          | 0.6          |
| Allolithocholate              | 2.3          | 0.6          |
| Epiallolithocholate           | 1.6          | 3            |
| 5-cholenic acid-3 $\beta$ -ol | 3.2          | 0.7          |

RMSD, root mean square deviation.

likely that this domain represents or at least contributes to the LC binding site (17). We proposed that the LC-target interaction required the steroid to insert normally to the bilayer plane: the hydrophobic hemisphere of the planar amphiphile faces the bilayer lipids while the hemisphere containing the polar hydroxyl faces polar amino acids provided by the  $\beta_1$ -subunit, with the carboxylate/carboxylic acid of the lateral chain residing in or near the aqueous solution (6, 17). If this model is correct, substitution of highly ionized groups for the polar hydroxyl group should decrease steroid insertion in the bilayer and, thus, reduce steroid access to the putative target site. Indeed, application of 150  $\mu\text{M}$  5 $\beta$ -cholanolic acid-3 $\alpha$ -sulfate (LCsulfate or compound 6 in Fig. 1) to the cytosolic side of I/O patches caused an increase in BK NPo that was significantly smaller than that evoked by LC (LCsulfate  $E_{\text{max}}/\text{LC } E_{\text{max}} = 0.59$ ), with NPo in LCsulfate reaching 153% of control (Fig. 5A, C; see supplementary Fig. II).

Negatively charged lipids are very effective activators of BK channels, with sulfo derivatives even surpassing activation by analogs containing carboxyls in equivalent positions in the molecule (e.g., tetradecasulfonate vs. myristic acid) (31). In the case of negatively charged FAs, BK channel activation does not require accessory  $\beta$  subunits, with the channel-forming  $\alpha$  being sufficient. Thus, to determine whether  $\alpha$  ("cbv1") +  $\beta_1$  channel response to LCsulfate could be explained by an action of this highly charged derivative on the channel  $\alpha$  subunit, we probed LCsulfate on homomeric cbv1 channel function. Cbv1 channels, however, remained insensitive to concentrations of LCsulfate as high as 300  $\mu\text{M}$  (see supplementary Fig. III). This result strongly suggests that LCsulfate effect on cbv1 +  $\beta_1$  requires the presence of the accessory subunit, as LC does. Thus, the reduced efficacy of LCsulfate is probably determined by the reduced penetration of the bilayer core by LCsulfate molecules.

Finally, to further test our insertion model, we reasoned that suppression of charge in the carboxylate of the bile acid lateral chain should diminish the solubility and/or insertion of the ionized group in the aqueous phase and, thus, diminish channel activation by these steroids. Therefore, we probed 5 $\beta$ -cholanolic acid 3 $\alpha$ -ol methyl ester (methylLC or compound 7 in Fig. 1), which contains a polar yet nonionized group at the end of the lateral chain. As expected, 150  $\mu\text{M}$  methylLC caused a very slight increase in BK channel NPo, not exceeding 123% of control (Fig. 5B, C).

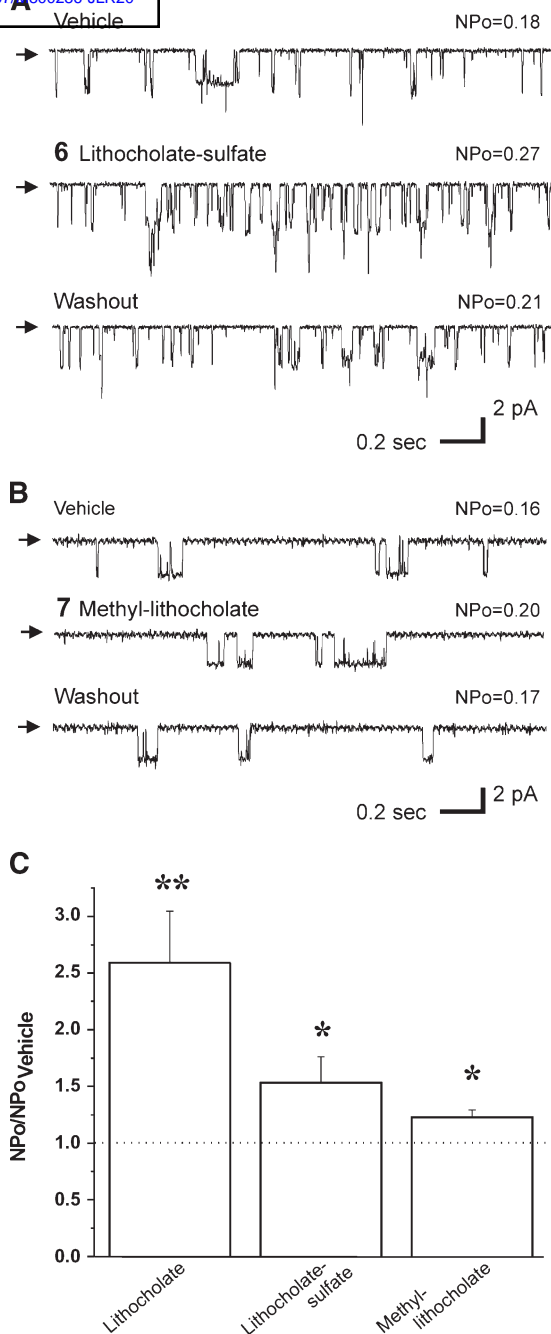


Fig. 5. LCsulfate and methylLC barely modify cbv1 +  $\beta_1$  channel activity. Representative single-channel records from I/O patches in the presence of 150  $\mu\text{M}$  LCsulfate (A) or methylLC (B), and respective vehicle-containing controls. All records were obtained at  $V_m = -20$  mV in symmetric  $\text{Ca}^{2+} = 10$   $\mu\text{M}$ . Arrows indicate baseline. C: Averaged channel responses to LC, LCsulfate, and methylLC. \*  $P < 0.05$  or \*\*  $P < 0.01$  vs. vehicle-containing solution;  $n = 6$  (LC),  $n = 6$  (LCsulfate), and  $n = 5$  (methylLC). Error bars indicate SEM.

Having explored the contribution of A/B *cis* junction bend,  $\alpha$  conformation of the hydroxyl group, steroidal hydrophobic concavity, and polarity of the lateral chain to recombinant BK channel activation by monohydroxylated bile acids, and having advanced that the  $\beta_1$  TM2 contributes to the LC binding pocket (6, 17), we used molecular dynamics simulations to model the LC- $\beta_1$  TM2 interaction.

The primary amino acid sequence of the  $\beta_1$  TM2 domain was modeled three-dimensionally as an ideal  $\alpha$ -helix. Our electrophysiological data indicate that the presence of the C3 hydroxyl group in an  $\alpha$ -configuration is critical for LC to cause robust channel activation (Figs. 2, 3), and earlier electrophysiological results are consistent with the ionized lateral chain end of the bile acid molecule residing in the aqueous medium and/or at the aqueous-bilayer interface (6). Based on the minimum energy conformation of LC as a bean-shaped molecule (Fig. 4A), we computed that the distance between LC functional groups, located at C3 and C24, is  $\approx 10.57$  Å. Therefore, we inferred that the polar residues of TM2  $\beta_1$ , which could provide interacting sites for the LC hydroxyl and carboxylate, should be located no more than 10–12 Å from the bilayer-aqueous interface. In addition, we showed that  $\beta_4$  subunits could not render the BK channel complex sensitive to LC, as  $\beta_1$  subunits did (6). Primary alignment of  $\beta_1$  and  $\beta_4$  subunits reveals the existence of two polar residues unique to the  $\beta_1$  TM2: T165 and T169 (see supplementary Fig. IV). Notably, both are located at a distance of no more than 12 Å from the bilayer-aqueous interface, an ideal location for any of these residues to hydrogen bond with the LC C3  $\alpha$  hydroxyl, having the bile acid inserted in the membrane almost normally to the bilayer plane.

Whether T165, T169, or both residues are interacting with the LC C3  $\alpha$  hydroxyl, such interaction(s) requires TM2 to fill the hydrophobic cleft underneath the hydrophobic rings of the LC concave hemisphere (Fig. 4A). Thus, we hypothesized two nonmutually exclusive regions in the  $\beta_1$  TM2 that may serve as LC-docking areas: 1) if  $\beta_1$  T169 interacts with the LC C3  $\alpha$  hydroxyl, L172 and L173 are strategically suited to fill the LC hydrophobic cleft; 2) if  $\beta_1$  T165 interacts with the LC C3  $\alpha$  hydroxyl, L161 would fill the hydrophobic cleft. Molecular dynamics simulations (see Methods) confirmed that LC interaction with either of these two docking areas may, indeed, occur (Fig. 6): in the “165/161 model,” the carboxylate (predominantly ionized) in the side chain of LC resides in or near the *extracellular* aqueous compartment (Fig. 6, A); in the “169/172/173 model,” the ionized carboxylate in the side chain of LC resides in or near the *cytosolic* aqueous compartment (Fig. 6, B).

As a first step in testing the validity of our general model, we decided to introduce mutations into  $\beta_1$  TM2 that should affect the effective interactions between the docking area and LC functional groups. Thus, we constructed the mutant T169A,K179A $\beta_1$ , which was coexpressed with *cbv1* to probe LC action. Considering the free movable nature of the LC lateral chain, the K179A mutation was included to prevent K179, located at the aqueous face near the lipid membrane, from stabilizing the LC carboxylate/carboxylic acid (see Fig. 6B and Discussion). An uncharged LC can still interact with K179 by hydrogen bonding rather than ion pairing (as the carboxylate does). Under recording conditions identical to those used in our LC studies on *cbv1*+ $\beta_1$  channels, LC potentiation of channel function was drastically blunted in channels containing  $\beta_1$  subunits with the double mutation (see supplementary Fig. VA, B), buttressing the idea that the  $\alpha$  hydroxyl (with some possible

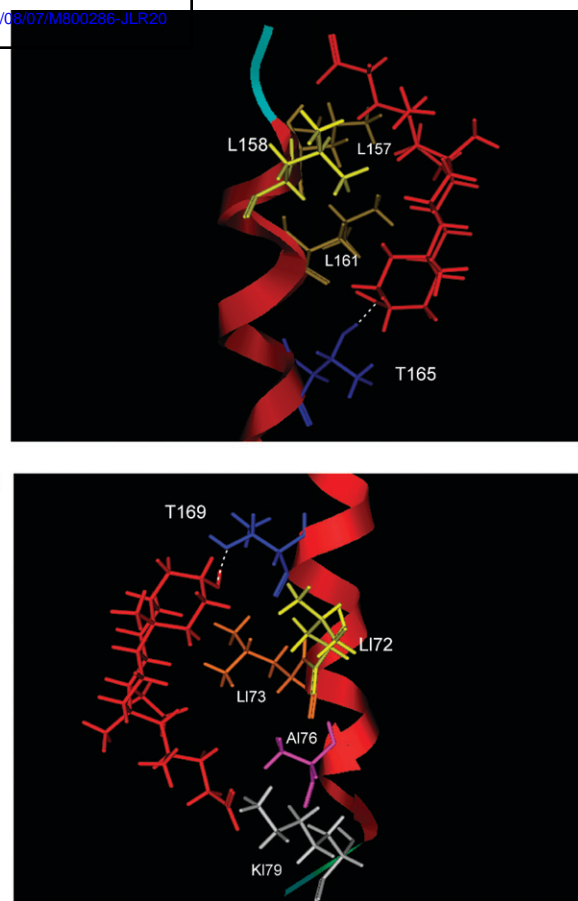


**Fig. 6.** Putative models for LC docking on the BK  $\beta_1$  subunit transmembrane domain 2 (TM2). Molecular dynamics simulation (see Methods) indicates that LC interaction with one or two distinct regions in the channel  $\beta_1$  subunit TM2 may occur. In the “165/161 model” the ionized carboxylate in the side chain of LC resides in or near the *extracellular* aqueous compartment (A), whereas in the “169/172/173 model” the ionized carboxylate in the side chain of LC resides in or near the *cytosolic* aqueous compartment (B). The TM2  $\alpha$  helix is shown in red, whereas peptide backbone near the aqueous face is shown in pale blue (A) and green (B); selected  $\beta_1$  amino acids are shown in colors: T (dark blue), L (different types of yellow), A (purple), and K (light gray); LC is shown in red.

contribution from the carboxylate) in LC interacts with the TM2 169/172/173 docking area. The channel with the mutated  $\beta_1$ , however, was somewhat responsive to LC ( $\leq 25\%$  increase in NPo over control values) (see supplementary Fig. VB). The simplest explanation is that the poor activation results from an impaired interaction between LC and the mutated 169/172/173 docking area. However, it may also reflect weak LC interactions via the 165/161 model (secondary or not to the mutations in 169/172/173), and/or interactions between nonionized bile acids with a site(s) anywhere else in the channel complex and its immediate lipidic microenvironment.

## DISCUSSION

Vasodilation caused by an increase in bile acid levels in systemic circulation is a major determinant of the systemic



hypotension associated with porto-systemic shunting that may occur in hepatobiliary disease (32). In hepatobiliary disease, not only overall increase in systemic bile acid levels but also changes in composition may occur, with drastic increase in LC levels (11). LC causes endothelium-independent relaxation of small arteries via activation of myocyte BK channels (6), a bile acid action that requires LC sensing by the channel  $\beta_1$  TM2 domain (17). Remarkably, among naturally occurring bile acids, LC is the most effective activator of vascular myocyte native BK channels (4). Our current study pinpoints the combination of a *cis* junction between steroidal rings A and B and the  $\alpha$  configuration of the C3 hydroxyl in the LC molecule as the key features that lead to robust channel activation. This combination imprints a bean shape to the LC molecule, with two clear-cut hemispheres: a convex, hydrophobic ( $\beta$ ) and a concave, hydrophilic ( $\alpha$ ) side, which stresses the distinct planar polarity of bile acids. Planar polarity ensures insertion of LC almost normally to the bilayer plane, making possible direct binding of the polar groups and the hydrophobic cleft that defines the concave side of LC with several polar and hydrophobic amino acids in  $\beta_1$  TM2.

Direct bile acid interactions with proteins and polypeptides require distinct chemical bonding between the steroid molecule and the peptide, with specificity and saturation in ligand action (as reviewed in Ref. 33; see also: 34–36). Indeed, all active bile acids that we tested fulfill these criteria (Figs. 2–4). Moreover, LC analogs that cannot meet LC steric requirements fail to modify BK channel activity (Figs. 2–4B), and analogs that can only meet these requirements partially, activate the BK channel with reduced effectiveness (Figs. 2–4A). Indeed, the relative efficacy of the various monohydroxylated bile acids in activating BK channels is related to the steroid capability to adopt the LC shape (Fig. 4; see supplementary Fig. I). These results, together with computer dynamics data of LC docking into defined  $\beta_1$  TM2 regions (Fig. 6), buttress the idea that BK channel activation is a result of direct binding of bile acid molecules to BK  $\beta_1$  TM2. While slo and BK  $\beta_{2-4}$  subunits are widely expressed,  $\beta_1$  subunits are highly abundant in smooth muscle and scarcely found in other tissues (16, 37). Therefore, pinpointing the structural features in LC and BK  $\beta_1$  TM2 leading to channel activation provides critical information for using LC as a template in designing BK channel modulators that selectively target the smooth muscle.

The simplest explanation for our data is that channel activation results from a direct interaction between bile acid monomers and  $\beta_1$  TM2, as advanced in our two docking models (Fig. 6). It is still possible, however, that LC monomers or small aggregates in the aqueous phase access the membrane and, once incorporated into the bilayer, form mixed micelles with lipids such as cholesterol. If so, sequestration of cholesterol from the channel environment could result in increased  $P_o$ , because cholesterol is a well-known inhibitor of BK channels (38–40). Several pieces of evidence make this possibility unlikely. First, incubation with deoxycholate at concentrations that increase smooth muscle BK channel activity, i.e., 100  $\mu$ M (4), fails to modify cholesterol or phospholipid content of

rat aorta smooth muscle membranes (7). Second, LC itself does not decrease but actually increases the cholesterol/phospholipid ratio of red blood cell membranes (41). Finally, LC activation of  $cbv1+\beta_1$  channels remains when studied on channels reconstituted into cholesterol-free phospholipid bilayers (17).


Although we favor a bile acid monomer- $\beta_1$  TM2 interaction(s), we cannot dismiss the possibility that LC could insert into the membrane as dimers or small aggregates and, as such, interact with the channel protein. A preferred form of bile acid insertion into membranes is as small aggregates consisting of two to four molecules of bile acids with their hydrophilic sides facing inwards, bound by hydrogen bonds between the hydroxyl groups (18, 42, 43). The pattern of bile acid effectiveness on BK channel function (cholate < deoxycholate < LC) argues against the possibility that channel activation results from channel protein interactions with this type of bile acid oligomer, as discussed in detail elsewhere (4). It is still possible, however, that the interaction with the channel protein involves small LC aggregates formed by a hydrophobic pairing between the convex planes (19, 28). If so, some LC molecules in the aggregate would be forced to expose their hydroxyl groups to the bilayer core, unless another domain of the BK channel (e.g., the channel  $\alpha$  subunit,  $\beta_1$  TM1, or even TM2 from another  $\beta_1$  subunit within the channel complex), some yet-to-be-identified BK-associated membrane protein, and/or some endogenous polar lipid provide stabilization. It should be noted, however, that LC-induced activation of  $cbv1+\beta_1$  channels incorporated into artificial POPE-POPS (3:1; w/w) bilayers is similar to that observed in native cell membranes ( $\approx 3$  times increase in channel  $P_o$ ) (17), strongly suggesting that a complex proteolipid environment is not necessary for LC-BK  $\beta_1$  interactions.

Whether in monomeric or small aggregate form, the planar and rigid nature of bile acids allows these steroids to insert into the membrane and reach the  $\beta_1$  TM2 domain with their steroidal nucleus deep in the bilayer while the lateral chain with its charged carboxyl remains at the water-lipid interface. Several results support this model of insertion. 1) Activation of smooth muscle BK channels by naturally occurring bile acids is a direct function of the steroid nucleus hydrophobicity (4), which is directly related to the bile acid capacity to partition in the bilayer core. Ursocholic acid, however, being more hydrophobic than LC, routinely failed to activate BK channels when applied to the cytosolic side of I/O patches (4), probably because of its lack of C3 hydroxyl to interact with polar regions in the  $\beta_1$  TM2 surface. 2) LC sulfate fails to activate  $cbv1+\beta_1$  channels (Fig. 5A, C). The  $pK_a$  of the sulfate is  $\sim 1-2$ , making it highly unlikely that this analog interdigitates in the bilayer core and accesses the proper docking regions (Fig. 6). 3) Channel activation was reduced by neutralization of negative charge in the lateral chain (Fig. 5B, C), which decreases the solubility of the polar chain in the aqueous phase. This loss of activity is consistent with the reduced activation of native BK channels when the end group of the bile acid lateral chain is made less polar [ $CH_2.OH$  or  $CO.OCH_3$  vs.  $CO.O^-$  in a series of cholate derivatives

(4)]. 4) BK channel activation is not dependent on a fixed length of the bile acid lateral chain (4), consistent with a freely movable chain in the aqueous phase.

Several steroids other than bile acids have been reported to increase BK NPo, including 17 $\beta$ -estradiol, xenoestrogens, androgens, and gluco- and mineralocorticoids. None of these steroids, however, appear to require the specific presence of  $\beta_1$  subunits for activating the channel (5, 44, 45), as LC does (6). Compared with other lipids and steroids, bile acids distinctly possess a unique bean shape and physicochemical properties (18). Our data indicate that BK channel activation directly relates to the capability of the steroid molecule to mimic the shape of LC (Table 2), supporting the contention that the molecular shape and planar polarity of bile acids are the essential features that allow these steroids to induce conformational changes in  $\beta_1$  TM2 that result in increased BK channel activity. Indeed, our molecular modeling data indicate that the LC molecule is energetically stable when it assumes the bean-shaped structure, with distinctive hydrophilic, concave and hydrophobic, convex hemispheres (Fig. 4A). This finding is in consonance with crystallographic data of sodium cholate monohydrate (46), a hydrophobic bile acid that shares with LC all basic structural features: steroidal nucleus with the C3 hydroxyl in the concave plane and an A/B *cis* junction (18, 19).

Based on bile acid monomer shape (Fig. 4) and molecular dynamics simulations of the  $\beta_1$  TM2, which acts as the BK channel LC sensor (17), we advance two docking models for LC. The first, which requires LC insertion from the extracellular side of the membrane, involves T165 forming a hydrogen bond with the LC C3 hydroxyl, a hydrophobic cleft that includes L161 stabilizing the LC hydrophobic steroidal nucleus, and L158 and L157 supporting the LC lateral chain (Fig. 6, top). This model agrees with a recently reported model of bile acid docking onto the farnesoid-X receptor, which also requires the presence of two hydrophobic amino acids (two phenylalanines) to interact with the bile acid steroid system (35). The second model, which requires LC insertion from the intracellular side of the membrane, involves T169 interacting via hydrogen bonding with the LC C3 hydroxyl, L172 and L173 providing the hydrophobic cleft for the LC nucleus, and A176 and K179 (Fig. 6, bottom) stabilizing the LC lateral chain, whether the latter includes a carboxylate or an unionized carboxylic acid. In the first model, however, the position of L158 and L157 will prevent interactions of LC derivatives with bulky lateral chains, and thus, it is more sterically restricted. In spite of small differences, both models provide complementary shapes and hydrogen bonding partners for LC, with epiLC and alloLC showing lower efficacy due to their different shape. Even when the C3 hydroxyls of these two analogs could be successfully positioned to hydrogen bond with T165 or T169, the position of methyl groups caused by the upside-down orientation adopted by epiLC and alloLC to match the LC shape (Fig. 4A) would alter their ability to stabilize the same conformation of the proposed binding areas, resulting in diminished channel activation (Figs. 2, 3).

The overall validity of our models is buttressed by the fact that LC action is drastically reduced when probed on channels including T169A, K179A $\beta_1$  subunits, underscoring the requirement of an intact 169/172/173/179 docking site for full LC effectiveness. Alanine scanning mutagenesis followed by substitution by amino acid residues varying in physicochemical properties such as molecular volume, length, and polarity, will help to determine the separate or concerted contribution of each docking area to bile acid action on BK channels. Notably, tauroLC, a compound that can effectively flip-flop across membranes only after several minutes (47), is equally effective to readily (<1 s) activate vascular myocyte native BK channels when applied either from the extracellular or intracellular leaflet of the membrane (4). These data suggest that the models for bile acid docking into and activation of BK channels are not mutually exclusive. However, considering the poor LC action on channels that contain T169A, K179A $\beta_1$  subunits, it is likely that extracellularly applied tauroLC, after being built up in the extracellular leaflet of the membrane (42), modulates BK channel function via a different, "fatty acid" site. This yet-to-be-identified site was reported for native pulmonary artery smooth muscle channels (made of  $\alpha + \beta_1$  subunits), being accessible solely from the extracellular medium (31, 48). 

The authors thank Dr. Daniel Baker (University of Memphis, Memphis, TN) for probing the purity of 5 $\alpha$ -cholanic acid 3 $\beta$ -ol by mass spectrometry, Dr. Alan Hofmann (University of California, La Jolla, CA) for valuable advice concerning handling of cholate derivatives, and Maria Asuncion-Chin (The University of Tennessee Health Science Center) for excellent technical assistance.

## REFERENCES

1. Brayden, J. E., and M. T. Nelson. 1992. Regulation of arterial tone by activation of calcium-dependent potassium channels. *Science*. **256**: 532–535.
2. Jaggar, J. H., G. C. Wellman, T. J. Heppner, V. A. Porter, G. J. Perez, M. Gollasch, T. Kleppisch, M. Rubart, A. S. Stevenson, W. J. Lederer, et al. 1998. Ca<sup>2+</sup> channels, ryanodine receptors and Ca(2+)-activated K<sup>+</sup> channels: a functional unit for regulating arterial tone. *Acta Physiol. Scand.* **164**: 577–587.
3. Valverde, M. A., P. Rojas, J. Amigo, D. Cosmelli, P. Orio, M. I. Bahamonde, G. E. Mann, C. Vergara, and R. Latorre. 1999. Acute activation of Maxi-K channels (hSlo) by estradiol binding to the beta subunit. *Science*. **285**: 1859–1860.
4. Dopico, A. M., J. V. Walsh, Jr., and J. J. Singer. 2002. Natural bile acids and synthetic analogues modulate large conductance Ca<sup>2+</sup>-activated K<sup>+</sup> (BKCa) channel activity in smooth muscle cells. *J. Gen. Physiol.* **119**: 251–273.
5. King, J. T., P. V. Lovell, M. Rishniw, M. I. Kotlikoff, M. L. Zeeman, and D. P. McCobb. 2006. Beta2 and beta4 subunits of BK channels confer differential sensitivity to acute modulation by steroid hormones. *J. Neurophysiol.* **95**: 2878–2888.
6. Bukiya, A. N., J. Liu, L. Toro, and A. M. Dopico. 2007. Beta1 (KCNMB1) subunits mediate lithocholate activation of large-conductance Ca<sup>2+</sup>-activated K<sup>+</sup> channels and dilation in small, resistance-size arteries. *Mol. Pharmacol.* **72**: 359–369.
7. Bomzon, A., and P. Ljubuncic. 1995. Bile acids as endogenous vasodilators? *Biochem. Pharmacol.* **49**: 581–589.
8. Lewis, B., D. Panveliwalla, S. Tabaqchali, and I. D. Wootton. 1969. Serum bile acids in intestinal disorders. *J. Physiol.* **202**: 46P.
9. Bomzon, A., J. P. Finberg, D. Tovbin, S. G. Naidu, and O. S. Better.

1984. Bile salts, hypotension and obstructive jaundice. *Clin. Sci. (Lond.)*. **67**: 177–183.
10. Tarantino, G., S. Cambri, A. Ferrara, M. Marzano, A. Liberti, G. Vellone, and A. F. Ciccarelli. 1989. Serum concentration of bile acids and portal hypertension in cirrhotic patients. Possible correlations. *Riv. Eur. Sci. Med. Farmacol.* **11**: 195–205.
11. Greco, A. V., and G. Mingrone. 1993. Serum bile acid concentrations in mild liver cirrhosis. *Clin. Chim. Acta.* **221**: 183–189.
12. Hamdan, H., and N. H. Stacey. 1993. Mechanism of trichloroethylene-induced elevation of individual serum bile acids. I. Correlation of trichloroethylene concentrations to bile acids in rat serum. *Toxicol. Appl. Pharmacol.* **121**: 291–295.
13. Ohkubo, H., K. Okuda, S. Iida, K. Ohnishi, S. Ikawa, and I. Makino. 1984. Role of portal and splenic vein shunts and impaired hepatic extraction in the elevated serum bile acids in liver cirrhosis. *Gastroenterology*. **86**: 514–520.
14. Ceryak, S., B. Bouscarel, and H. Fromm. 1993. Comparative binding of bile acids to serum lipoproteins and albumin. *J. Lipid Res.* **34**: 1661–1674.
15. Ljubuncic, P., O. Said, Y. Ehrlich, J. Meddings, E. Shaffer, and A. Bomzon. 2000. On the in vitro vasoactivity of bile acids. *Br. J. Pharmacol.* **131**: 387–398.
16. Brenner, R., T. J. Jegla, A. Wickenden, Y. Liu, and R. W. Aldrich. 2000. Cloning and functional characterization of novel large conductance calcium-activated potassium channel beta subunits, hKCNMB3 and hKCNMB4. *J. Biol. Chem.* **275**: 6453–6461.
17. Bukiya, A., T. Vaithianathan, L. Toro, and A. Dopico. 2008. The second transmembrane domain of the large conductance, voltage- and calcium-gated potassium channel  $\beta_1$  subunit is a lithocholate sensor. *FEBS Lett.* **582**: 673–678.
18. Carey, M. 1985. Physical-chemical properties of bile acids and their salts. In *Sterols and Bile Acids*. H. Danielsson and J. Sjovall, editors. Elsevier Science Publishers, Amsterdam, Netherlands. 345–403.
19. Miyajima, K., K. Machida, T. Taga, H. Komatsu, and M. Nakagaki. 1988. Correlation between the hydrophobic nature of monosaccharides and cholates and their hydrophobic indices. *J. Chem. Soc., Faraday Trans.* **84**: 2537–2544.
20. Dopico, A., V. Anantharam, and S. Treistman. 1998. Ethanol increases the activity of  $\text{Ca}^{2+}$ -dependent  $\text{K}^+$  (mslo) channels: functional interaction with cytosolic  $\text{Ca}^{2+}$ . *J. Pharmacol. Exp. Ther.* **284**: 258–268.
21. Liu, J., T. Vaithianathan, K. Manivannan, A. Parrill, and A. M. Dopico. 2008. Ethanol modulates BKCa channels by acting as an adjuvant of calcium. *Mol. Pharmacol.* **74**: 628–640.
22. Halgren, T. A. 1996. Merck Molecular Force Field. *J. Comput. Chem.* **17**: 490–641.
23. Wang, J., P. Cieplak, and P. A. Kollman. 2000. How well does a restrained electrostatic potential (RESP) model perform in calculating conformational energies of organic and biological molecules? *J. Comput. Chem.* **21**: 1049–1074.
24. Cornell, B. A., G. Krishna, P. D. Osman, R. D. Pace, and L. Wiczorek. 2001. Tethered-bilayer lipid membranes as a support for membrane-active peptides. *Biochem. Soc. Trans.* **29**: 613–617.
25. Knot, H. J., and M. Nelson. 1998. Regulation of arterial diameter and wall  $[\text{Ca}^{2+}]$  in cerebral arteries of rat by membrane potential and intravascular pressure. *J. Physiol.* **508**: 199–209.
26. Perez, G. J., A. D. Bonev, and M. T. Nelson. 2001. Micromolar  $\text{Ca}^{2+}$  from sparks activates  $\text{Ca}^{2+}$ -sensitive  $\text{K}^+$  channels in rat cerebral artery smooth muscle. *Am. J. Physiol. Cell Physiol.* **281**: C1769–C1775.
27. Roda, A., A. F. Hoffman, and K. J. Mysels. 1983. The influence of bile salt structure on self-association in aqueous solutions. *J. Biol. Chem.* **258**: 6362–6370.
28. Carey, M. C., and D. M. Small. 1972. Micelle formation by bile salts. Physical-chemical and thermodynamic considerations. *Arch. Intern. Med.* **130**: 506–527.
29. Ko, J., J. A. Hamilton, H. T. Ton-Nu, C. D. Schteingart, A. F. Hofmann, and D. M. Small. 1994. Effects of side chain length on ionization behavior and transbilayer transport of unconjugated dihydroxy bile acids: a comparison of nor-chenodeoxycholic acid and chenodeoxycholic acid. *J. Lipid Res.* **35**: 883–892.
30. Cabral, D. J., J. A. Hamilton, and D. M. Small. 1986. The ionization behavior of bile acids in different aqueous environments. *J. Lipid Res.* **27**: 334–343.
31. Clarke, A. L., S. Petrou, J. V. Walsh, Jr., and J. J. Singer. 2002. Modulation of BK(Ca) channel activity by fatty acids: structural requirements and mechanism of action. *Am. J. Physiol. Cell Physiol.* **283**: C1441–C1453.
32. Pak, J. M., and S. S. Lee. 1993. Vasoactive effects of bile salts in cirrhotic rats: in vivo and in vitro studies. *Hepatology*. **18**: 1175–1181.
33. Stolz, A. H., M. Takikawa, M. Ookhtens, and N. Kaplowitz. 1989. The role of cytoplasmic proteins in hepatic bile acid transport. *Annu. Rev. Physiol.* **51**: 161–176.
34. Mizushima, Y., N. Kasai, K. Miura, S. Hanashima, M. Takemura, H. Yoshida, F. Sugawara, and K. Sakaguchi. 2004. Structural relationship of lithocholic acid derivatives binding to the N-terminal 8-kDa domain of DNA polymerase beta. *Biochemistry*. **43**: 10669–10677.
35. Katona, B. W., C. L. Cummins, A. D. Ferguson, T. Li, D. R. Schmidt, D. J. Mangelsdorf, and D. F. Covey. 2007. Synthesis, characterization, and receptor interaction profiles of enantiomeric bile acids. *J. Med. Chem.* **50**: 6048–6058.
36. Ishizawa, M., M. Matsunawa, R. Adachi, S. Uno, K. Ikeda, H. Masuno, M. Shimizu, K. I. Iwasaki, S. Yamada, and M. Makishima. 2008. Lithocholic acid derivatives act as selective vitamin D receptor modulators without inducing hypercalcemia. *J. Lipid Res.* **49**: 763–772.
37. Orio, P., P. Rojas, G. Ferreira, and R. Latorre. 2002. New disguises for an old channel: MaxiK channel beta-subunits. *News Physiol. Sci.* **17**: 156–161.
38. Bolotina, V., V. Omelyanenko, B. Heyes, U. Ryan, and P. Bregestovski. 1989. Variations of membrane cholesterol alter the kinetics of  $\text{Ca}^{2+}$ -dependent  $\text{K}^+$  channels and membrane fluidity in vascular smooth muscle cells. *Pflugers Arch.* **415**: 262–268.
39. Chang, H. M., R. Reitsstetter, R. P. Mason, and R. Gruener. 1995. Attenuation of channel kinetics and conductance by cholesterol: an interpretation using structural stress as a unifying concept. *J. Membr. Biol.* **143**: 51–63.
40. Crowley, J. J., S. N. Treistman, and A. M. Dopico. 2005. Distinct structural features of phospholipids differentially determine ethanol sensitivity and basal function of BK channels. *Mol. Pharmacol.* **68**: 4–10.
41. Balistreri, W. F., M. H. Leslie, and R. A. Cooper. 1981. Increased cholesterol and decreased fluidity of red blood cell membranes (spur cell anemia) in progressive intrahepatic cholestasis. *Pediatrics*. **67**: 461–466.
42. Schubert, R., K. Beyer, H. Wolburg, and K-H. Schmidt. 1986. Structural changes in membranes of large unilamellar vesicles after binding of sodium cholate. *Biochemistry*. **25**: 5263–5269.
43. Schubert, R., and K. H. Schmidt. 1988. Structural changes in vesicle membranes and mixed micelles of various lipid compositions after binding of different bile salts. *Biochemistry*. **27**: 8787–8794.
44. Korovkina, V. P., A. M. Brainard, P. Ismail, T. Schmidt, and S. England. 2004. Estradiol binding to maxi-K channels induces their down-regulation via proteasomal degradation. *J. Biol. Chem.* **279**: 1217–1223.
45. Duncan, R. K. 2005. Tamoxifen alters gating of the BK alpha subunit and mediates enhanced interactions with the avian beta subunit. *Biochem. Pharmacol.* **70**: 47–58.
46. Cobbleddick, R. L., and F. W. Einstein. 1980. The structure of sodium  $3\alpha, 7\alpha, 12\alpha$ -trihydroxy- $5\beta$ -cholan-24-oate monohydrate (sodium cholate monohydrate). *Acta Crystallogr. B*. **36**: 287–292.
47. Kamp, F., J. A. Hamilton, F. Kamp, H. V. Westerhoff, and J. A. Hamilton. 1993. Movement of fatty acids, fatty acid analogues, and bile acids across phospholipid bilayers. *Biochemistry*. **32**: 11074–11086.
48. Clarke, A. L., S. Petrou, J. V. Walsh, Jr., and J. J. Singer. 2003. Site of action of fatty acids and other charged lipids on BKCa channels from arterial smooth muscle cells. *Am. J. Physiol. Cell Physiol.* **284**: C607–C619.